

# Detection of pulse trains in the electrically stimulated cochlea: Effects of cochlear health<sup>a)</sup>

Bryan E. Pfungst,<sup>b)</sup> Deborah J. Colesa, Sheena Hembrador, Stephen Y. Kang, John C. Middlebrooks,<sup>c)</sup> Yehoash Raphael, and Gina L. Su  
*Kresge Hearing Research Institute, Department of Otolaryngology, University of Michigan, 1150 West Medical Center Drive, Ann Arbor, Michigan 48109-5616*

(Received 20 March 2011; revised 13 September 2011; accepted 14 September 2011)

Perception of electrical stimuli varies widely across users of cochlear implants and across stimulation sites in individual users. It is commonly assumed that the ability of subjects to detect and discriminate electrical signals is dependent, in part, on conditions in the implanted cochlea, but evidence supporting that hypothesis is sparse. The objective of this study was to define specific relationships between the survival of tissues near the implanted electrodes and the functional responses to electrical stimulation of those electrodes. Psychophysical and neurophysiological procedures were used to assess stimulus detection as a function of pulse rate under the various degrees of cochlear pathology. Cochlear morphology, assessed *post-mortem*, ranged from near-normal numbers of hair cells, peripheral processes and spiral ganglion cells, to complete absence of hair cells and peripheral processes and small numbers of surviving spiral ganglion cells. The psychophysical and neurophysiological studies indicated that slopes and levels of the threshold versus pulse rate functions reflected multipulse integration throughout the 200 ms pulse train with an additional contribution of interactions between adjacent pulses at high pulse rates. The amount of multipulse integration was correlated with the health of the implanted cochlea with implications for perception of more complex prosthetic stimuli. © 2011 Acoustical Society of America.

[DOI: 10.1121/1.3651820]

PACS number(s): 43.66.Ts, 43.66.Cb, 43.64.Me [BLM]

Pages: 3954–3968

## I. INTRODUCTION

Perception of electrical stimuli varies considerably across users of cochlear implants (Munson and Nelson, 2005; Gfeller *et al.*, 2008; Wilson and Dorman, 2008). In addition, psychophysical measures of detection and discrimination of electrical stimuli show considerable variation across stimulation sites within individual implants (Donaldson *et al.*, 1997; Pfungst and Xu, 2004; Bierer, 2007; Pfungst *et al.*, 2008). It is commonly assumed that this variation in perception is due in part to variation in cochlear pathology across subjects and along the length of the implanted cochlea within subjects. However, the details of the relationships between this pathology and perception are poorly understood. Animal models in which the conditions in the implanted cochlea can be determined histologically within a short time after obtaining psychophysical or physiological data can reveal details of how conditions in the implanted ear affect the perception of cochlear implant stimulation.

One hypothesized effect of cochlear pathology is that loss or dysfunction of neural elements leads to higher detection thresholds for cochlear implant stimulation. However, previous studies have shown that the relationship between survival of hair cells and auditory neurons and psychophys-

ical detection thresholds depends on the parameters of stimulation (Su *et al.*, 2008; Kang *et al.*, 2010). The relationship is positive for some types of stimuli and negative for others.

The experiments reported here focused on detection thresholds for trains of short-duration (20 or 25  $\mu$ s/phase) pulses. Such pulse trains are the carrier signals for most current cochlear implant stimulation strategies. The pulse rates in these carrier pulse trains affect information transfer and perception with cochlear implants as assessed by psychophysical and neurophysiological measures. Carrier rates greater than 1000 pulses per second (pps) can result in degraded modulation detection and increased channel interaction compared to results with lower carrier rates (Middlebrooks, 2004, 2008; Galvin and Fu, 2005, 2009; Pfungst *et al.*, 2007).

In a study of cortical neuronal-spike responses to cochlear implant stimulation in neomycin-deafened anesthetized guinea pigs, Middlebrooks (2004) compared thresholds as a function of pulse rate for pulse rates below 1000 pps with those for rates above 1000 pps. For short-duration pulses, above 1000 pps where interpulse intervals (IPIs) were short (<1 ms), there was evidence for the influence of one sub-threshold pulse lowering the threshold of one or more succeeding pulses (Middlebrooks, 2004). This was probably due to incomplete recovery from partial depolarization following the first pulse. Such partial depolarization would then sum across pulses to lower the threshold for the pulse train. In contrast, below 1000 pps the pulses are sufficiently separated in time to allow complete recovery from the first sub-threshold pulse before the second pulse is delivered. The study demonstrated that cortical-spike thresholds were relatively constant as a function of pulse rate at rates below 1000 pps.

<sup>a)</sup>Portions of this work were presented at the Midwinter Meeting of the Association for Research in Otolaryngology, February 2010.

<sup>b)</sup>Author to whom correspondence should be addressed. Electronic mail: bpfungst@umich.edu.

<sup>c)</sup>Current address: Department of Otolaryngology, University of California at Irvine, Room 404D, Medical Sciences D, Irvine, CA 92697-5310.

In a study of psychophysical detection thresholds in guinea pigs, Kang and colleagues (2010) also found that, for cochlear implants in neomycin-deafened chronically implanted ears, slopes of threshold versus pulse rate functions were very shallow at pulse rates below 1000 pps and that thresholds decreased as a function of pulse rate at pulse rates above 1000 pps. These results were very similar to those obtained by Middlebrooks (2004) in the cortical studies. However, for animals that were implanted in a hearing ear with no predeafening, a strikingly different result was obtained. In these cases, slopes of threshold versus pulse rate functions were typically negative at rates above and below 1000 pps. In these cases, some acoustic hearing was often preserved and auditory-nerve survival was typically much better than that in ears where slopes were very shallow or zero at rates below 1000 pps (Kang *et al.*, 2010).

The present study was aimed at elucidating the mechanisms underlying the effects of pulse rate on detection thresholds and the interaction of these mechanisms with pathology in the implanted ear. We hypothesized that two mechanisms underlie the effects of pulse rate on detection thresholds: A temporal multipulse integration mechanism and a residual partial-depolarization mechanism. Temporal integration of multiple pulses and other stimulus waveforms typically occurs over stimulus durations up to approximately 300 ms in both acoustic and electrical hearing (Gerken *et al.*, 1990; Donaldson *et al.*, 1997) resulting in lower thresholds for longer duration stimuli. A similar mechanism could apply to the 200 ms pulse trains studied by Kang and colleagues (2010) because the number of pulses in the 200 ms train increased as a function of pulse rate. The residual partial-depolarization mechanism was described by Middlebrooks (2004): Residual partial depolarization from one pulse summates with partial depolarization in a subsequent pulse to facilitate neural discharge at lower current levels. This mechanism requires high pulse rates where IPIs are less than about 1 ms.

From experiments in humans in our laboratory and elsewhere (e.g., Donaldson *et al.*, 1997; Zhou *et al.*, 2011), it is known that the slopes of threshold-versus-pulse-rate and threshold-versus-pulse-train-duration functions vary across stimulation sites within individual subjects. These data suggest that temporal multipulse integration depends in part on conditions in the implanted cochlea close to the stimulation sites. To test this hypothesis we compared the slopes of these functions to various measures of cochlear health in the region of the implanted electrode array in guinea pigs.

## II. METHOD

### A. Overview

Subjects for all experiments were adult male guinea pigs obtained from the Elm Hill breeding facility (Chemsford, MA). The animals were trained using positive reinforcement operant conditioning techniques to perform a go/no-go psychophysical task that was used to assess detection threshold levels for acoustic and electrical stimuli. After being trained to respond to threshold- and suprathreshold-level acoustic stimuli, all of the animals were implanted in one ear with a Nucleus animal implant obtained from Coch-

lear, Ltd. (Lane Cove, Australia). Two animals (guinea pigs 436 and 411) had implant failures after starting the experiments and were reimplanted in the same ear. In both of these cases, the data presented here are for the second implant.

The cochlear implant consisted of 8 platinum-band electrodes on a silicone rubber carrier. The electrodes were spaced at intervals of approximately 0.75 mm center to center. The implant was inserted into the basal half turn of the scala tympani through a cochleostomy made approximately 0.7 mm apical to the round window. Typically only the apical five or six electrodes could be inserted into the scala tympani. The narrowing of the scala tympani in the second half of the basal turn prevented the tip of the implant, which was ~0.4 mm diameter, from advancing further. The electrodes were labeled A through F starting at the apical end of the electrode array. Most of the experiments were conducted using monopolar stimulation of electrode B. In two cases, one or more electrode connections were broken and electrodes C (animal 419) or E (animal 408) were used for data collection. Electrical stimuli consisted of trains of symmetric biphasic pulses with phase durations of 20 or 25  $\mu$ s and no interphase gap.

The animals were divided into two treatment groups. One group received cochlear implants in a hearing ear that had no treatment before implantation. In this group, the contralateral ear was deafened by scala tympani injection of neomycin so that hearing in the implanted ear could be tested with no contribution from the contralateral ear. Deafening of this contralateral ear took place several weeks or months prior to implantation of the test ear.

The second group was deafened in the implanted ear with a 10% neomycin sulfate solution (60  $\mu$ l) injected into the scala tympani just prior to implantation. In this group, the contralateral ear had a variety of conditions: three were neomycin deafened, two were hearing ears implanted with cochlear implants that failed prior to the inclusion of the animals in these experiments, and one had normal hearing.

Key dependent variables in this study included slopes of plots of detection thresholds as a function of pulse rate, interpulse interval, or stimulus duration. For threshold versus pulse rate functions, slopes were calculated separately for pulse rates below 1000 pps and rates above 1000 pps. All slopes were calculated based on linear best-fit regression lines. Chi-square goodness of fit values were all less than or equal to 1 (median = 0.08, interquartile range = 0.01–0.25) indicating that the linear regression lines were a good fit to the data.

In these studies considerable variability across animals was observed in the amount of acoustic hearing preservation, hair-cell preservation and nerve survival in the guinea pigs implanted in hearing ears<sup>1</sup> whereas the neomycin-deafened ears typically showed no acoustic hearing, no ABR, no inner hair cell survival, and sparse spiral ganglion cell survival.

We report the experiments and results in three parts. In part I we report on psychophysical experiments designed to elucidate the mechanisms underlying the effects of pulse rate on thresholds and the effects of implantation and deafening procedures on these mechanisms. In part II, we report on experiments in which cortical-spike data were obtained in acute recording sessions following the collection of the psychophysical data. In part III, we compare the slopes of

TABLE I. Summary of the research design.

Part	Number of Subjects per Treatment Group	Purpose of Experiment and Stimulus Parameters
I-A	Hearing Implanted = 7 Deaf Implanted = 6	Determine effects of pulse rate and interpulse interval on thresholds over a wide range of pulse rates. (200 ms pulse trains at 5 pps to 5000 pps)
I-B		Determine the effects of pulse separation in the absence of effects of pulse number. (2-pulse stimuli with IPI = 0.2 ms to 200 ms)
I-C	Hearing Implanted = 2 Deaf Implanted = 3	Determine the effect of number of pulses per stimulus in the absence of changes in interpulse interval by varying pulse-train duration. (1 to 256 pulses at 400 pps)
II	Hearing Implanted = 2 Deaf Implanted = 4	Compare pulse rate functions for psychophysical thresholds versus thresholds of neurons in primary auditory cortex. (200 ms pulse trains at 156 to 5000 pps)
III	Hearing Implanted = 19 Deaf Implanted = 9	Compare histology and physiology results with the slopes of pulse rate functions. (data from multiple studies)

threshold versus pulse rate functions with various measures of nerve survival and function. For part III we include animals from parts I and II and animals from the Kang *et al.* (2010) study. Only animals from which we had obtained both functional and histological data were used for part III.

The three parts of the study are summarized in Table I. Details are given in the following sections.

## B. Part I

Psychophysical detection threshold functions were examined under three conditions. (A) To determine the effects of pulse rate and interpulse interval on the detection of pulse trains over a large range of pulse rates, 200 ms pulse trains with pulse rates from 5 pps (IPI = 200 ms yielding a single biphasic pulse) to 5000 pps (IPI = 0.2 ms) were used. (B) To determine the effects of pulse separation in the absence of effects of number of pulses in the stimulus, two-pulse stimuli were used with interpulse intervals ranging from 0.2 to 200 ms. (C) To determine the relationship of detection of multiple pulses in the absence of changes in interpulse interval, threshold versus stimulus duration functions were examined with pulse rate held constant at 400 pps. Pulses per stimulus ranged from 1 to 256 pulses as the pulse train duration ranged from 2.5 to 640 ms. Thirteen animals completed parts I-A and I-B. Seven were implanted in a hearing ear and six were implanted in a neomycin-deafened ear. The data for parts I-A and I-B were collected at the same time, with the conditions for these two parts being tested in random order. A subset of this group of animals completed part I-C after the completion of parts I-A and I-B.

Animals for part I ( $n = 13$ ) were trained using positive reinforcement operant conditioning procedures. The animals were trained to initiate a trial by depressing a button on the floor of the test cage, waiting for a variable period (1–6 s) until they detected the onset of an auditory signal, and releasing the button if they detected the signal. Correct detections were rewarded with a food pellet (Purina Test Diets). The method of constant stimuli was used with stimulus levels ranging from subthreshold to suprathreshold. Psy-

chometric functions were obtained using 15 to 20 trials per stimulus level and threshold was defined as the level at which detections were indicated on 50% of the trials.

In addition to psychophysical detection thresholds for electrical pulses, several other measures were obtained for the animals in part I. Acoustic detection thresholds were obtained in the animals that were implanted without predeafening. These animals were all deafened in the contralateral ear by local perfusion of neomycin, and hearing in the implanted ear was measured using free-field stimulation from a speaker located above the animal's cage. The acoustic thresholds were assessed prior to implantation and periodically throughout the testing with electrical stimulation. The acoustic stimuli were 200 ms tone bursts at frequencies of 8, 16, and 24 kHz. Rise and fall times were 10 to 15 ms.

Ensemble spontaneous activity (ESA) in the auditory nerve was assessed by recording electrical activity in the cochlea at the electrode used for the psychophysical data collection. In most cases, recordings were made approximately one month after implantation and again toward the end of the experiment. The electrical activity was recorded in the absence of any electrical or intentional acoustic stimulation. Recordings were made under anesthesia with the animals in a sound-attenuating chamber. The electrical signals were then analyzed using the methods developed by Dolan *et al.* (1990) and Searchfield *et al.* (2004) and summarized in Kang *et al.* (2010).<sup>2</sup> These studies have associated a peak in the spectrum near 900 Hz with spontaneous activity in the auditory nerve. The recorded signal was subjected to spectral analysis and the spectrum was then examined to determine the peak voltage in the range from 422 Hz to 1203 Hz and the frequency at which it occurred.

After completion of all psychophysical and physiological measurements, at times after implantation ranging from 4 to 18 months (mean of 12 months), the animals from part I were deeply anesthetized and prepared for histological analysis. Three normal untreated control ears were also analyzed to assess normal appearance of hair cells and auditory neurons in the analysis region.

The procedures used for intracardial perfusion and histological processing were similar to those used in the Kang

*et al.* (2010) study. Briefly, following perfusion, temporal bones from both sides were extracted and decalcified. The cochlea was decalcified until the electrode array was visible. At that point, the location of the electrode used for the psychophysical and electrophysiological data collection (usually electrode B), was determined and a notch in the bony wall of the cochlea was made at that site using a needle. The implant was then removed and the cochlea was embedded in JB-4 resin (Electron Microscopy Scientific, Washington, PA, USA). Forty sections on the para-midmodiolar plane were taken beginning at the site of the notch. Sections 3  $\mu\text{m}$  thick were collected and stained with 1% toluidine blue in 1% sodium borate. The sections encompassed 120  $\mu\text{m}$  of the cochlear spiral, a distance thought to be within the 300  $\mu\text{m}$  width of the electrode of interest. In the contralateral ear, sections at a comparable location were collected.

One person, blinded to the identity of the subjects, carried out the histological analysis. Of the 40 sections saved (numbered 1–40) from each ear, five were analyzed. Section selection began with a randomly chosen section from the first eight sections. Every eighth section after that was used. This protocol was applied to maintain adequate spacing between sections so as to prevent counting the same cell more than once. The information collected from each of the five slides was then averaged and for each ear studied, a mean inner hair cell (IHC) count, mean outer hair cell (OHC) count, spiral ganglion neuron (SGN) packing density and a ranking of the amount of visible peripheral processes (PP) of the spiral ganglion neurons were determined.

Each para-midmodiolar section contained eight profiles of the organ of Corti and six profiles of Rosenthal's canal. For this study, the four most basal profiles were examined as detailed in the Results section for part I. The implanted electrode array was located in the scala tympani in the most basal profile.

Inner hair cells (IHCs) were counted only if the nucleus and stereocilia were observed, in order to avoid counting the same cell twice. The mosaic pattern of the outer hair cells (OHCs) did not allow all parts of the cells to be seen in any of the 3  $\mu\text{m}$  para-midmodiolar sections so OHCs were counted as present if any part of the cell was seen. To calculate the percentage of hair cells present compared to normal, mean IHC counts of each section were divided by 1 and mean OHC counts by 3. All SGN cells with cell bodies of 12–25  $\mu\text{m}$  in diameter and nuclei of 5–9  $\mu\text{m}$  in diameter were counted. SGN packing density (cells/mm<sup>2</sup>) was calculated after determining the cross-sectional area of Rosenthal's canal using an ImageJ computerized image-analysis system. Quantitative analysis of the PPs was not possible, but instead the fibers were ranked on a scale of visually estimated quantity with 0 being none and 3 being high. Morphological conditions similar to those seen in the current study are illustrated in Kang *et al.* (2010).

### C. Part II

A separate group of animals was used to determine the relationship between psychophysical and cortical-neurophysiological responses under various stimulus and subject condi-

tions. Six animals completed this part. Two were implanted in a hearing ear and four were implanted in an ear deafened by local perfusion of neomycin. Psychophysical detection threshold versus pulse rate functions were obtained, after which the animals were anesthetized and cortical extracellular-neural-spike threshold versus pulse rate functions were obtained for the same stimulus parameters.

Psychophysical procedures used in part II were the same as those used in part I except that the stimulus set was smaller. Psychophysical threshold versus pulse rate functions for 200 ms pulse trains were tested over a range of pulse rates from 156 to 5000 pps.

After the completion of the psychophysical threshold testing at times ranging from 5 to 21 months post implantation, extracellular spike waveforms of neurons in primary auditory cortex were recorded in response to monopolar cochlear-implant stimulation. Procedures for these acute recording sessions were identical to those detailed in Middlebrooks (2004). Briefly, animals were anesthetized throughout surgical and data-collection periods with ketamine and xylazine. Extracellular spike waveforms were recorded from cortical area A1 using 16-site silicon-substrate recording probes (NeuroNexus Technologies), and single- and multi-unit spikes were detected with off-line analysis of recorded waveforms. Thresholds for cortical responses to electrical cochlear stimulation were derived from trial-by-trial analysis of spike counts using a signal-detection procedure described by Middlebrooks and Snyder (2007). Of the animals in part II, histological analysis was performed only on animal 317.

### D. Part III

In part III of this report we compare functional and histological measures for 28 animals. These include the 13 animals from part I, 1 animal from part II and 14 animals from Kang *et al.* (2010). The psychophysical, electrophysiological and histological procedures were as described in part I above except that for part II of this study and for the Kang *et al.* (2010) study the lowest pulse rate tested was 156 pps.

## III. RESULTS

### A. Part I—Psychophysical, electrophysiological and histological results

The seven animals from part I that were implanted in a hearing ear had various degrees of preserved acoustic hearing (Fig. 1). The contralateral (nonimplanted) ears of these animals were deafened by local perfusion of neomycin and no hair cells were found in those ears, as detailed below. Therefore, the residual hearing in these animals is reasonably attributed to conditions in the implanted ear. Four of the seven animals had preserved hearing in the implanted ear at all three tested frequencies (8, 16, and 24 kHz) throughout the experiment. In these animals, thresholds shortly after implantation were usually high relative to pre-implantation thresholds. Then there was usually a decrease in thresholds (increase in acoustic sensitivity) over the first week after implantation, followed by a period of relative stability for several months and then sometimes an increase in thresholds.

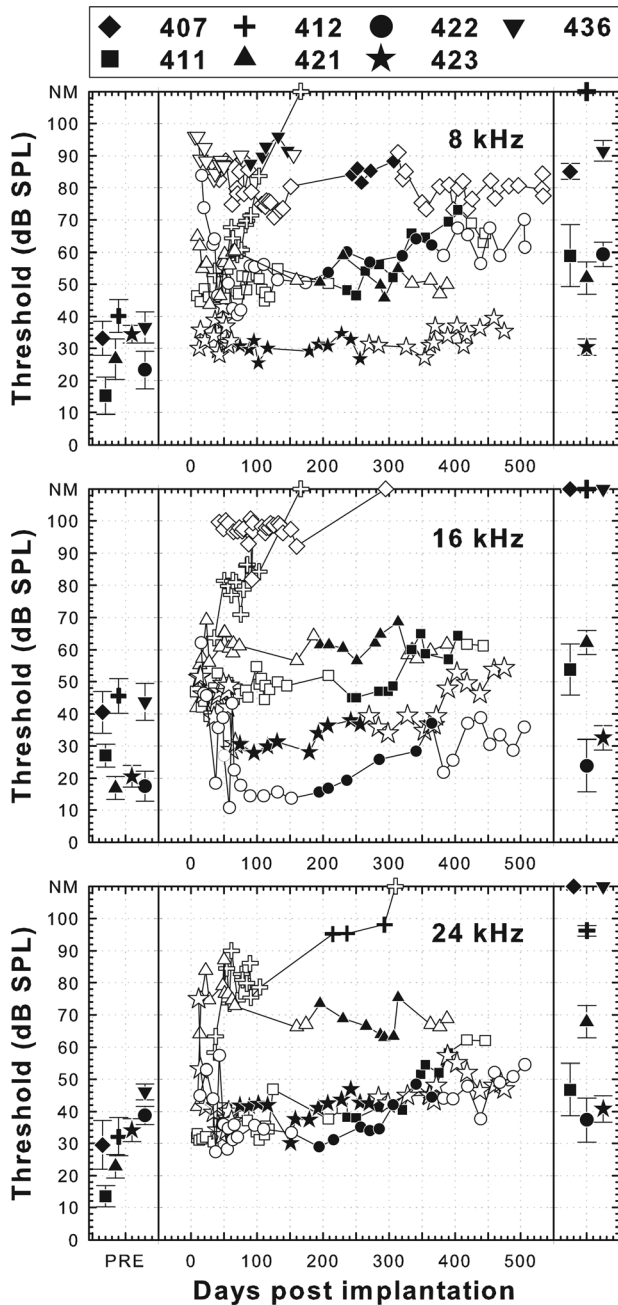


FIG. 1. Psychophysical pure-tone detection thresholds in the implanted ear prior to implantation, and as a function of time after implantation, for animals implanted in a hearing ear. The contralateral ear had been deafened with neomycin in all cases. The left column shows the mean and standard deviation of the last 10 thresholds collected before implantation. The middle column shows the thresholds as a function of time after implantation. Filled symbols in the middle column indicate acoustic thresholds measured during the time period when the electrical threshold versus pulse rate functions shown in Figs. 2 and 3 were being collected. The right-hand column shows the means and standard deviations of these values. Open symbols in the middle column indicate acoustic thresholds obtained before and after this period. NM indicates that thresholds could not be measured within the limits of our sound systems. Symbol shapes for these seven animals are maintained as filled black symbols through the remainder of the figures.

The remaining three animals in this group showed relatively high acoustic thresholds after implantation and thresholds at one or more of the tested frequencies increased over time to unmeasurable levels (Fig. 1).

TABLE II. Insertion depths from the round window to the center of the electrode used for data collection in part I, and the corresponding tonotopic locations.

Subject	Electrode Insertion Depth Estimate (mm)	Center Frequency Estimate* (kHz)
407	2.9	20
411	3.8	16
412	1.7	28
422	3.9	16
423	2.7	22
436	3.4	18
<b>Mean Implanted Hearing Ears</b>	<b>3.0</b>	<b>20</b>
408	1.3	31
419	2.6	22
420	2.8	21
433	3.6	17
437	3.8	16
438	3.2	19
<b>Mean Implanted Deaf Ears</b>	<b>2.9</b>	<b>21</b>
<b>Mean All Ears except 421</b>	<b>3.0</b>	<b>21</b>

For the three animals that were deafened with neomycin perfusion in both ears, deafness was confirmed by acoustic testing. It is reasonable to assume that the animals that received neomycin infusion only in the implanted ear were completely deaf in that ear because no hair cells were found in that ear at the end of the experiment.

Insertion depths of the cochlear implant electrode arrays were estimated based on observations at the time of surgery and post-mortem examination of the dissected, decalcified temporal bones where the position of the electrodes could be observed directly. These data are shown in Table II. Electrode placement for animal 421 could not be specified due to a possible migration of the implant during histological preparation. For the remaining animals, the estimated insertion depths of the electrodes used for psychophysical and ESA testing ranged from 1.3 to 3.9 mm from the round window to the center of the electrode (mean = 3.0 mm; SD = 0.8 mm;  $n = 12$ ). Two of these animals had shallow insertion depths for the electrodes used for psychophysical data collection due either to failure of more apical electrodes (animal 408, electrode E at 1.3 mm was used) or shallow insertion of the electrode array (animal 412, electrode B was at 1.7 mm). For the

remaining 10 animals, the range was 2.6 to 3.9 mm (mean = 3.2 mm; SD = 0.5 mm). Based on the model of Greenwood (1990), we estimated the best frequency near the electrode used for data collection. These values ranged across all animals from 16 to 31 kHz with a mean of approximately 21 kHz, or 19 kHz with the two shallow insertions excluded.

Psychophysical threshold versus pulse rate functions for cochlear implant stimulation varied across the 13 subjects from part I (Fig. 2). The slopes of these functions above and below 1000 pps were calculated separately based on linear best-fit regression lines. At pulse rates below 1000 pps, slopes ranged from  $-0.24$  to  $-1.96$  dB per doubling of pulse rate (a factor of 8) and above 1000 pps they ranged from  $-0.27$  to  $-4.25$  dB per doubling (a factor of 15). Slopes at pulse rates above 1000 pps were steeper than those below 1000 pps in all cases except for animal 436 [Fig. 2(B)].

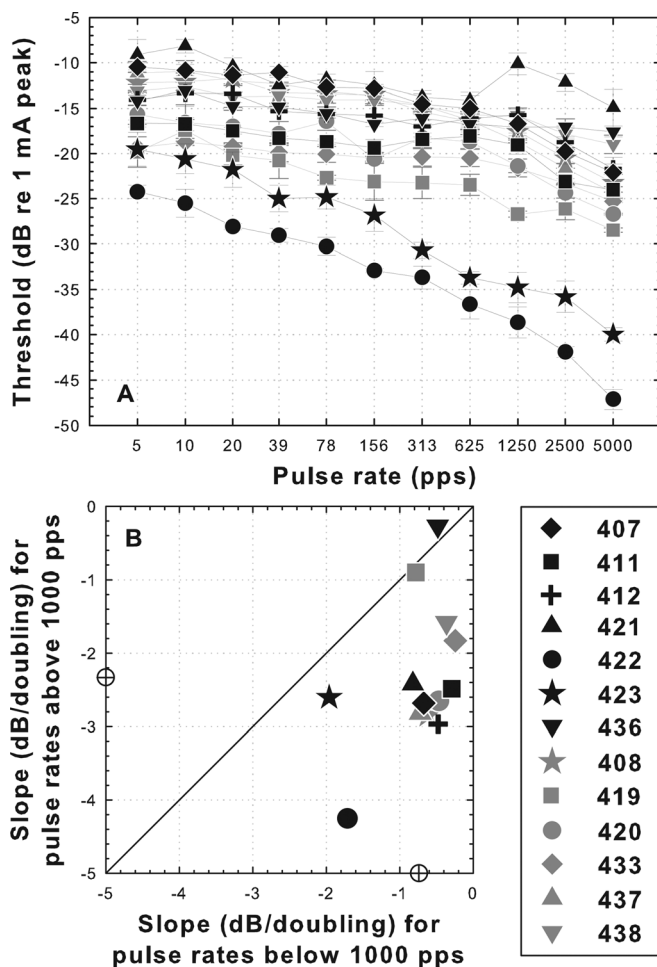


FIG. 2. Psychophysical electrical detection thresholds as a function of pulse rate for 200 ms electrical pulse trains for the 13 subjects from part I. Black symbols are for animals for which the implant was inserted in a hearing ear and gray symbols are for animals in which the ear was infused with neomycin prior to implantation. (A) Thresholds as a function of pulse rate. (B) Slopes of threshold versus pulse rate functions above 1000 pps versus slopes below 1000 pps. Slopes were calculated from linear best-fit regression lines. Points below the diagonal indicate that the slopes of the functions above 1000 pps were steeper (more negative) than slopes below 1000 pps. Mean slopes for all animals are indicated by open circles on the X and Y axes. Slopes above 1000 pps were significantly steeper than those below 1000 pps ( $t = 5.09, p < 0.0001$ ). Symbols identifying each animal are given in the legend and are maintained throughout the manuscript.

Across all animals, the mean slope above 1000 pps was significantly steeper than that below 1000 pps ( $t = 5.09, df = 24, p < 0.0001$ ).

For animals deafened with neomycin before implantation (gray symbols in Fig. 2), slopes of functions below 1000 pps were always shallower than  $-1$  dB per doubling (mean =  $-0.53$ ; range =  $-0.24$  to  $-0.78$ ). In contrast, two of the animals implanted in a hearing ear (animals 422 and 423; black circle and star in Fig. 2) showed steeper slopes below 1000 pps than any of the other animals ( $-1.71$  and  $-1.96$  dB/doubling; Fig. 2). These were the two animals that had the best preserved acoustic hearing at 16 kHz (Fig. 1). The remaining animals that were implanted in hearing ears (remaining black symbols in Fig. 1), including two with moderately preserved acoustic hearing, had slopes below 1000 pps that were similar to those of the neomycin-deafened animals (Fig. 2).

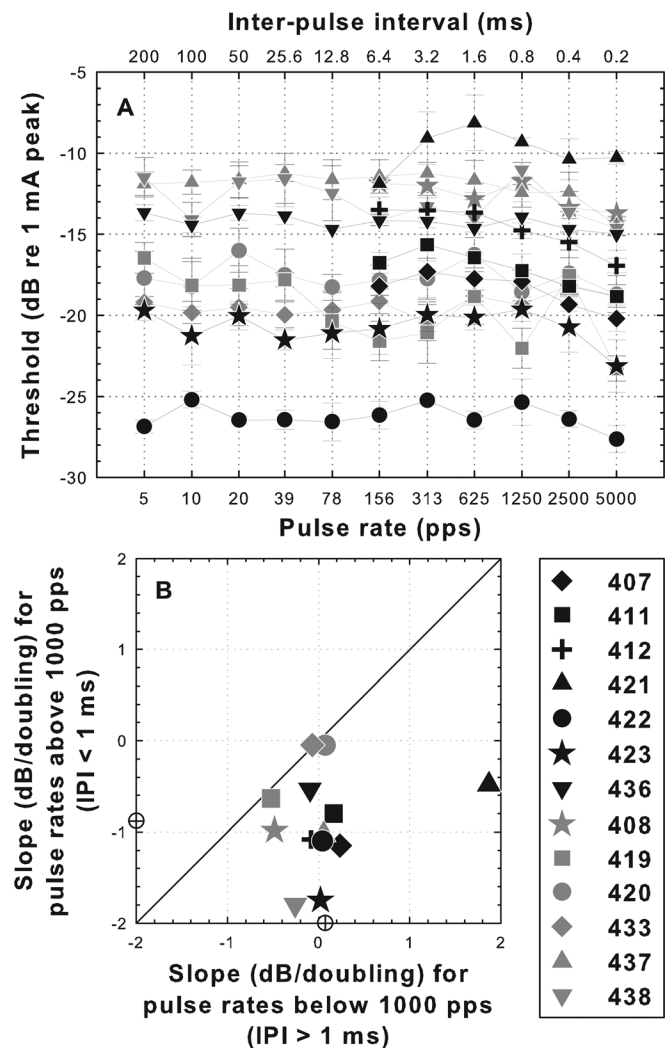


FIG. 3. (A) Psychophysical electrical detection thresholds as a function of pulse rate (lower abscissa) and inter-pulse interval (upper abscissa) for two-pulse stimuli for the 13 subjects from part I. (B) Slopes of threshold versus pulse rate functions above 1000 pps (IPI < 1 ms) versus slopes below 1000 pps (IPI > 1 ms). Points below the diagonal indicate that the slopes of the functions above 1000 pps were steeper (more negative) than slopes below 1000 pps. Mean slopes for all animals are indicated by open circles on the X and Y axes. Slopes above 1000 pps were significantly steeper than those below 1000 pps ( $t = 4.31, p = 0.0002$ ).

When the number of pulses per stimulus was held constant at two pulses, thresholds at rates below 1000 pps (IPI > 1 ms) showed little or no decrease as a function of pulse rate (1/IPI) (Fig. 3). Importantly, this included the two animals that had steep slopes in this region for 200 ms pulse trains [black star and circle; compare Figs. 2(A) and 3(A)]. Thus, interpulse interval had little or no effect on thresholds at pulse rates below 1000 pps. Above 1000 pps, slopes for the two-pulse stimuli were all negative although they were much shallower than the slopes for the 200 ms pulse trains above 1000 pps (mean of  $-0.82$  dB/doubling for the two-pulse stimuli versus  $-2.33$  dB/doubling for the 200 ms pulse trains). For the two-pulse stimuli, as for the 200 ms pulse trains, slopes above 1000 pps were significantly more negative than those below 1000 pps ( $t = 4.31$ ,  $df = 24$ ,  $p = 0.0002$ ).

The data for animals 422 and 423 in Figs. 2 and 3 suggest that the thresholds at pulse rates below 1000 pps were affected only by the number of pulses occurring in the stimulus and not the interpulse interval. To further examine the effects of number of pulses, thresholds were obtained when the pulse rate was held constant at 400 pps and duration of the stimulus (and

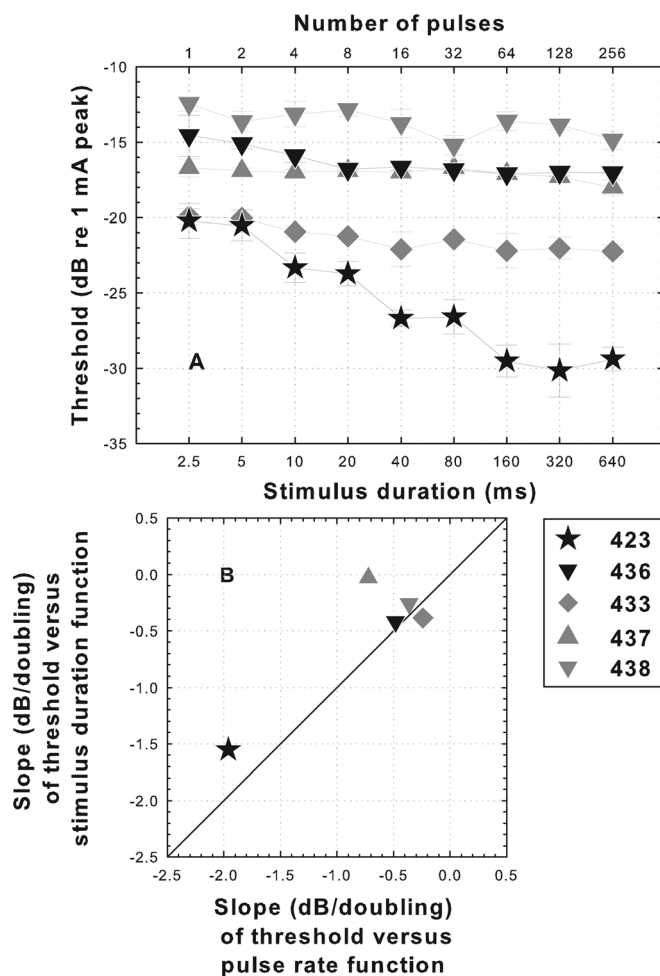


FIG. 4. (A) Psychophysical electrical detection thresholds as a function of stimulus duration (number of pulses per stimulus) when pulse rate was held constant at 400 pps. Data were obtained for a subset of the subjects shown in Figs. 2 and 3. (B) Scatter plot comparing slopes of threshold versus pulse rate functions (data from Fig. 2) with slopes of threshold versus stimulus duration functions [data from (A)] for the same subjects.

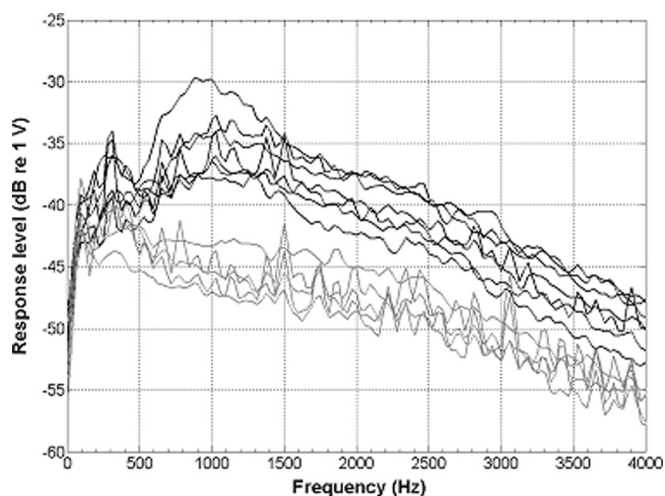


FIG. 5. Examples of ESA spectra for 12 of the 13 animals in part I. No data were obtained for animal 408. Black lines represent the seven animals implanted in a hearing ear and the gray lines represent five animals implanted in a deafened ear. Peak voltages near 900 Hz and the frequencies at which they were obtained are given in Table III.

thus the number of pulses in the stimulus) was varied. These data were collected for five of the subjects (Fig. 4). Across this group of subjects, the slopes of the threshold versus stimulus-duration functions were similar to the slopes of the threshold versus pulse rate functions [Fig. 4(B)]. Animal 423, which has a steep threshold versus pulse rate function also had a steep threshold versus stimulus duration function and the remaining cases had shallow slopes for both functions.

Spontaneous activity in the auditory nerve was estimated using ESA recordings (Dolan *et al.*, 1990; Searchfield *et al.*, 2004). Examples of the ESA spectra are shown in Fig. 5. All of the animals that were implanted in a hearing ear (black traces in Fig. 5) showed a peak in the ESA voltage spectrum in the analysis range (422 to 1203 Hz). These responses ranged from  $-41.4$  to  $-29.7$  dB re 1 V (Table III). ESA voltage spectra were assessed for 5 of the 6 animals that were treated with neomycin in the implanted ear, but none of these showed a peak response in the analysis region (gray traces in Fig. 5).

Morphology of the implanted cochleae was assessed shortly after all psychophysical and electrophysiological assessments were completed, at times ranging from 4 to 18 months after implantation. The degree of hair cell preservation and nerve survival varied greatly across the population of animals used in these experiments. Conditions in the basal region of the cochlea, in the region occupied by the implant, ranged from near-normal hair cells, peripheral processes and SGN packing densities to complete absence of hair cells and peripheral processes and low SGN densities. The most severe pathology was observed in the cochleae that were infused with neomycin prior to implantation. In animals that received cochlear implants in hearing ears, morphology differed considerably from case to case.

Histological data from the implanted ears of the 13 subjects from part I are shown in Fig. 6. The data in Fig. 6 show counts of hair cells, estimates of peripheral process survival, and SGN packing densities made from para-midmodiolar sections that were centered at the location of the electrode used for measurement of the psychophysical data shown in

TABLE III. Ensemble spontaneous activity (ESA) measurement results. Results obtained approximately 1 month (27 to 34 days) after implantation (“initial measurement”) and 161 to 535 days after implantation (“final measurement”) for the 7 animals from part I that were implanted in a hearing ear are shown in the top 7 rows. Animals deafened with neomycin in the implanted ear (bottom 5 rows) were tested only once. The frequency (Hz) at which the peak voltage occurred within the analysis window (422 to 1203 Hz) and the voltage level at that peak (dB re 1 V) are shown. Final ESA data were not obtained for subject 421 due to an implant failure. No ESA data were obtained for animal 408 (from the deafened group). Examples of waveforms are shown in Figure 5.

Subject	Initial Measurement		Final Measurement	
	Frequency at Peak (Hz)	Voltage at Peak (dB re 1 V)	Frequency at Peak (Hz)	Voltage at Peak (dB re 1 V)
407	968.8	-41.4	968.8	-36.6
411	906.3	-35.8	968.8	-34.2
412	968.8	-35.8	968.8	-37.1
421	906.3	-37.6		
422	906.3	-33.3	875.0	-29.7
423	875.0	-34.6	906.3	-34.2
436	968.8	-38.5	968.8	-37.1
419			531.3	-43.0
420			500.0	-45.3
433			468.8	-41.7
437	500.0	-41.9		
438	781.0	-41.3		

Figs. 2 through 4 and the ESA data shown in Fig. 5 and Table III. Data for four cross-sectional profiles are shown ranging from profile “a” at the basal turn in the region occupied by the implant and proceeding in an apical direction to profile “d” at the apical end of the second turn. Profiles “b” through “d” were apical to the implant. For animals 408 and 422, the temporal bones were partially damaged during histological preparation and only some of the cross-sectional profiles could be analyzed.

In profiles “a” and “b,” IHCs ranged from 20 to 100% of normal across the seven animals that were implanted in a hearing ear. Most of these ears showed greater than 75% IHC survival in profiles “c” and “d” with the notable exception of animal 436 who had no surviving IHCs in these apical turns despite 40% to 60% survival in profiles “a” and “b.” In animals deafened with neomycin in the implanted ear, no IHCs were seen in any turn.

OHC survival ranged from 0 to 100% in profiles “a” and “b” of the ears that were implanted without predeafening and was greater than 75% in profiles “c” and “d,” again with the exception of animal 436 (Fig. 6). No OHCs were found in any turn of the neomycin-deafened implanted ears.

Peripheral processes (PPs) of the spiral ganglion neurons could not be counted in detail in the para-midmodiolar sections, but their presence was estimated on a scale from 0 (none seen) to 3 (many seen). Some peripheral processes were present in profile “a” in all of the animals implanted in hearing ears and few or none were seen in the neomycin-deafened ears.

Spiral ganglion neuron cell-body packing density was estimated by counting all cells that had a diameter of 12 to 25  $\mu\text{m}$  and a nucleus with a diameter of 5 to 9  $\mu\text{m}$  and dividing by the cross-sectional area of Rosenthal’s canal. In the animals implanted in a hearing ear, SGN densities in profile “a” ranged from 275 cells/ $\text{mm}^2$  to 1103 cells/ $\text{mm}^2$  (near normal). In three animals with normal ears the SGN densities in profile “a” ranged from 1052 cells/ $\text{mm}^2$  to 1591 cells/ $\text{mm}^2$ . The mean SGN densities for these three normal ears for profiles “a” through “d” were 1338, 1084, 1107, and 1030 cells/ $\text{mm}^2$ , respectively.

In the neomycin treated, implanted ears, SGN densities in profile “a” ranged from 14 to 135 cells/ $\text{mm}^2$ .

In animals implanted in a hearing ear, the contralateral ears were deafened by perfusion of neomycin. The histology from these contralateral ears is shown by the open symbols in Fig. 6. In these ears, there were no hair cells, and SGN densities were very low (36 to 117 cells/ $\text{mm}^2$  in profile “a”).

In summary, all of the animals that were implanted in a hearing ear had moderate to good IHC survival and SGN survival in the region of the implant. Furthermore the variability of IHC and SGN survival across these animals was greater than that found in the animals in the study by Kang *et al.* (2010). Animals implanted in neomycin-deafened ears had no hair cells and lower SGN packing densities than any of the animals implanted in a hearing ear. The relationships between these histological measures and measures of cochlear implant function will be detailed in part III of this manuscript.

## B. Part II—Comparison of psychophysical and cortical measures

Psychophysical threshold versus pulse rate functions for the six animals from part II are shown in Fig. 7(A). As in part I of this study and in the Kang *et al.* (2010) study, the slopes of threshold versus pulse rate functions below 1000 pps for the four animals implanted in a neomycin-deafened ear were shallow with none being steeper than  $-1$  dB/doubling while the slopes for the two animals implanted in a hearing ear were of two types with the slope for animal 317 being steeper ( $-1.6$  dB/doubling) and that for animal 253 ( $+0.1$  dB/doubling) being similar to those for the deafened animals. The cortical-spike threshold versus pulse rate functions for these same animals are shown in Fig. 7(B). The slopes of the cortical-spike functions were similar to those of the psychophysical functions except that the slopes of the psychophysical functions were sometimes a little steeper [Fig. 7(C)].

## C. Part III—Comparison of functional and histological measures for combined studies

All of the measures of cochlear health taken in these experiments, with the exception of pure-tone thresholds,

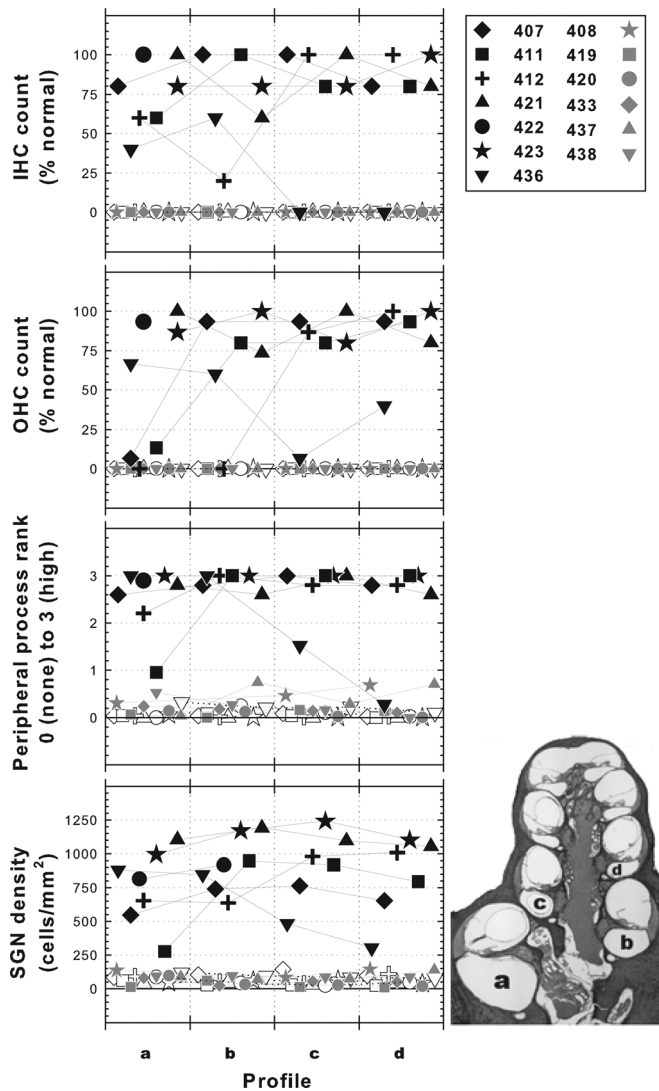


FIG. 6. Surviving hair cells, SGN peripheral processes (estimate), and SGN cell body density in each of four profiles from para-midmodiolar sections of each cochlea. The para-midmodiolar sections were centered at the location of the electrodes used for data collection. As illustrated in the lower right diagram, profile “a” was in the basal turn in the region occupied by the implant. Profile “b” was in the basal turn apical to the implant. Profiles “c” and “d” were in the second turn. Within each profile-section of the graph, data are scattered along the abscissa to avoid overlap of symbols. Data are for the 13 animals from part I of this study. The filled black symbols show data for the implanted ears of the seven animals that were implanted in hearing ears. The open symbols of the same shape are for the neomycin-deafened contralateral ears of these animals. The filled gray symbols are for the implanted ears in the six animals that had implants in a neomycin-deafened ear. For animals 408 and 422 there was some damage during histological processing of the implanted ears rendering some profiles unreadable, so only partial data are shown.

were significantly correlated with the slopes of the threshold versus pulse rate functions at pulse rates below 1000 pps (Fig. 8). For pure-tone thresholds, only animals with measurable hearing were included in the correlation analysis. There was one outlier in this group (animal 347). With this case removed, the correlation coefficient for 16 kHz acoustic thresholds with slopes of electrical threshold versus pulse rate functions below 1000 pps was 0.61 ( $p = 0.016$ ,  $n = 15$ ). Note that all of the anatomical and physiological measures

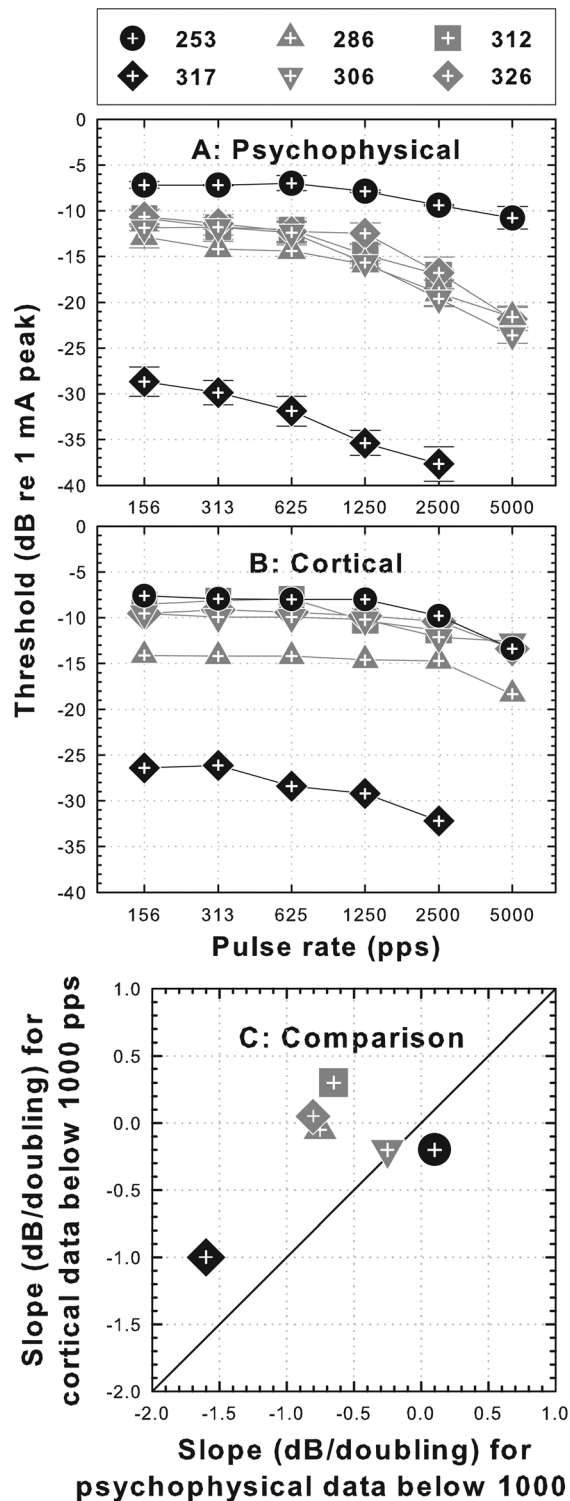


FIG. 7. Psychophysical and cortical threshold data for the six animals in part II of the study. Two animals that received implants in a hearing ear are represented by black symbols and the four animals that were deafened with neomycin in the implanted ear are represented by gray symbols. (A) Psychophysical detection threshold versus pulse rate functions. (B) Cortical-spike threshold versus pulse rate functions. (C) Comparison of psychophysical and cortical function slopes for pulse rates below 1000 pps.

used in Fig. 8 were also highly significantly correlated with each other (Table IV).

Of the anatomical and physiological measures of cochlear health considered in this study, the highest correlation with slopes of the threshold versus pulse rate functions

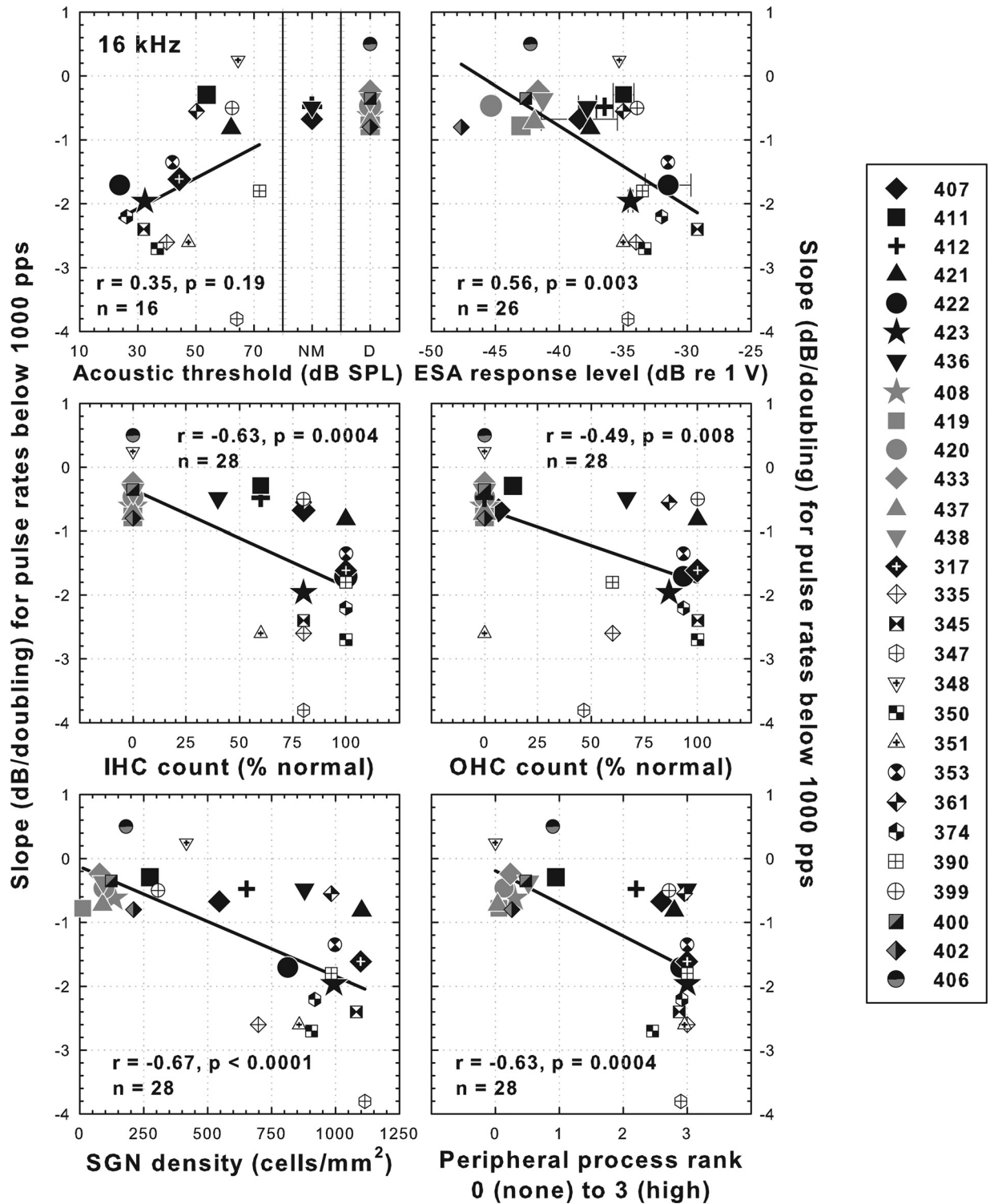


FIG. 8. Scatter plots comparing various measures of cochlear health with slopes of threshold versus pulse rate functions for 200 ms pulse trains at pulse rates below 1000 pps. Data are from 13 animals from part I of this study, one animal from part II and 14 animals from Kang *et al.* (2010). Symbols in black or black and white are for animals implanted in a hearing ear. Symbols in gray or black and gray are for animals implanted in an ear deafened by local perfusion of neomycin. Acoustic thresholds are the average values for 16 kHz tones measured during the time period when the electrical threshold versus pulse rate functions were being collected. ESA data show means and ranges in cases where two values were obtained. All histological data are from profile “a” as illustrated in Fig. 6, lower right diagram. Linear regression lines and correlation coefficients are shown. For acoustic detection thresholds (upper left panel) the regression line is based only on animals with measurable hearing. NM = no measurable hearing. D = deafened in the implanted ear with local perfusion of neomycin. Note ESA measurements (upper right panel) were performed in animals 408 and 317.

below 1000 pps was SGN packing density ( $r = 0.67$ ), but correlations with IHC and OHC count, estimates of peripheral process density and ESA voltages were also highly significant

(Fig. 8). Nevertheless, none of the cochlear-health measures were perfect predictors of the slopes of these psychophysical functions. For example, animals with slopes steeper than

TABLE IV. Correlations among the electrophysiological and histological measures of cochlear health used in Figures 8 and 9.

	IHC	OHC	SGN	PP
ESA	r = 0.84 p < 0.001 n = 26	r = 0.74 p < 0.001 n = 26	r = 0.78 p < 0.001 n = 26	r = 0.79 p < 0.001 n = 26
IHC		r = 0.83 p < 0.001 n = 28	r = 0.87 p < 0.001 n = 28	r = 0.92 p < 0.001 n = 28
OHC			r = 0.78 p < 0.001 n = 28	r = 0.79 p < 0.001 n = 28
SGN				r = 0.90 p < 0.001 n = 28

–1.0 dB/doubling all had SGN densities greater than 600 cells/mm<sup>2</sup>, but four animals with shallower slopes also had SGN densities greater than 600 cells/mm<sup>2</sup>.

Slopes of psychophysical threshold versus pulse rate functions at pulse rates above 1000 pps were less strongly correlated with any of the measures of cochlear health compared to the slopes below 1000 pps (compare Figs. 8 and 9). None of the correlations for pulse rates above 1000 pps were statistically significant at the  $p < 0.01$  level.

## IV. DISCUSSION

### A. Effects of pulse rate on psychophysical thresholds

The data presented in part I are consistent with the hypothesis that two mechanisms underlie the effects of pulse rate on psychophysical detection thresholds: (1) long term temporal multipulse integration based on the number of pulses in the 200 ms stimulus and (2) residual partial-depolarization from preceding subthreshold pulses that accumulates and lowers thresholds for following pulses.

Temporal integration was probably the cause of the steep slopes of the threshold versus pulse rate functions for the 200 ms pulse trains below 1000 pps for animals 422 and 423 in Fig. 2 and for many of the animals from a previous study (Kang *et al.*, 2010). The auditory system is known to integrate stimuli over a period of about 300 ms to achieve lower detection thresholds (Gerken *et al.*, 1990). For threshold versus pulse rate functions for the 200 ms pulse trains, the number of pulses within the 200 ms window increased, and thresholds decreased, as a function of pulse rate. Further support for the temporal integration interpretation comes from the experiment in which the number of pulses per stimulus was varied by holding pulse rate constant at 400 pps and varying the stimulus duration. In that case, we found that steepnesses of slopes of the threshold versus stimulus duration functions were similar across animals to the slopes of the threshold versus pulse rate functions [Fig. 4(B)].

The threshold versus pulse rate functions at rates above 1000 pps are attributed in part to the residual partial-

depolarization mechanism, based on the data and interpretation detailed in Middlebrooks (2004). For pulse rates greater than 1000 pps, we hypothesize that at current levels just below the threshold for neural discharge, one pulse partially depolarizes a neuron or group of neurons and subsequent pulses falling within a window of approximately 1 ms add to the partial depolarization, eventually resulting in neural action potentials. Higher pulse rates (with smaller interpulse intervals and more pulses falling within the 1 ms window), increase the probability of action potentials and lower the threshold level. However, below 1000 pps this mechanism is less likely to be effective because complete recovery from partial depolarization is expected to occur within about 1 ms. In the current experiment, decreases in threshold as a function of pulse rate for two animals occurred at very low pulse rates, down to 10 pps where interpulse intervals were 100 ms (Fig. 2), far too long to expect residual partial-depolarization from one pulse to affect the response to a subsequent pulse. Further evidence that the thresholds for pulse rates below 1000 pps were not affected by pulse interactions comes from the experiment with pulse pairs. Thresholds for pulse pairs as a function of pulse rate had slopes near zero in all cases, including the animals that had steep slopes for the 200 ms pulse trains [compare Figs. 2(A) and 3(A)]. At rates above 1000 pps, thresholds for the two-pulse stimuli did decrease as a function of pulse rate for most animals as expected. Exceptions were animals 420 and 433 where thresholds fluctuated as a function of pulse rate and did not show a clear decrease above 1000 pps.

Interestingly, above 1000 pps where interpulse intervals were less than 1 ms, the slopes of the threshold versus pulse rate functions for two-pulse stimuli, which averaged –0.82 dB per doubling, were much shallower than those for 200 ms pulse trains, where the slope averaged –2.33 dB per doubling [compare Figs. 2(A) and 3(A)]. A similar observation was made by Middlebrooks (2004). The most likely explanation for the flatter slopes in the 2-pulse condition is that increasing pulse rates in the 200-ms pulse-train condition produced both decreased interpulse intervals and more pulses within the 1 ms window following the first pulse, whereas increasing rates in the two-pulse condition produced only the shortened interpulse interval with no increase in the pulse count.

### B. Comparison of psychophysical and cortical physiological data

Case by case, the thresholds obtained from spike recording in the auditory cortex tended to correlate with psychophysical thresholds (Fig. 7). In particular, the extraordinarily low thresholds observed for animal 317 were observed both physiologically and psychophysically. Psychophysical and cortical results also agreed in showing a decrease in thresholds associated with increases in pulse rates above 1000 pps. These similarities suggest that many of the mechanisms affecting across-subject differences in the slopes and levels of the psychophysical functions are located in the auditory pathway at or below the level of the primary auditory cortex, and not at higher centers or non-auditory pathways.

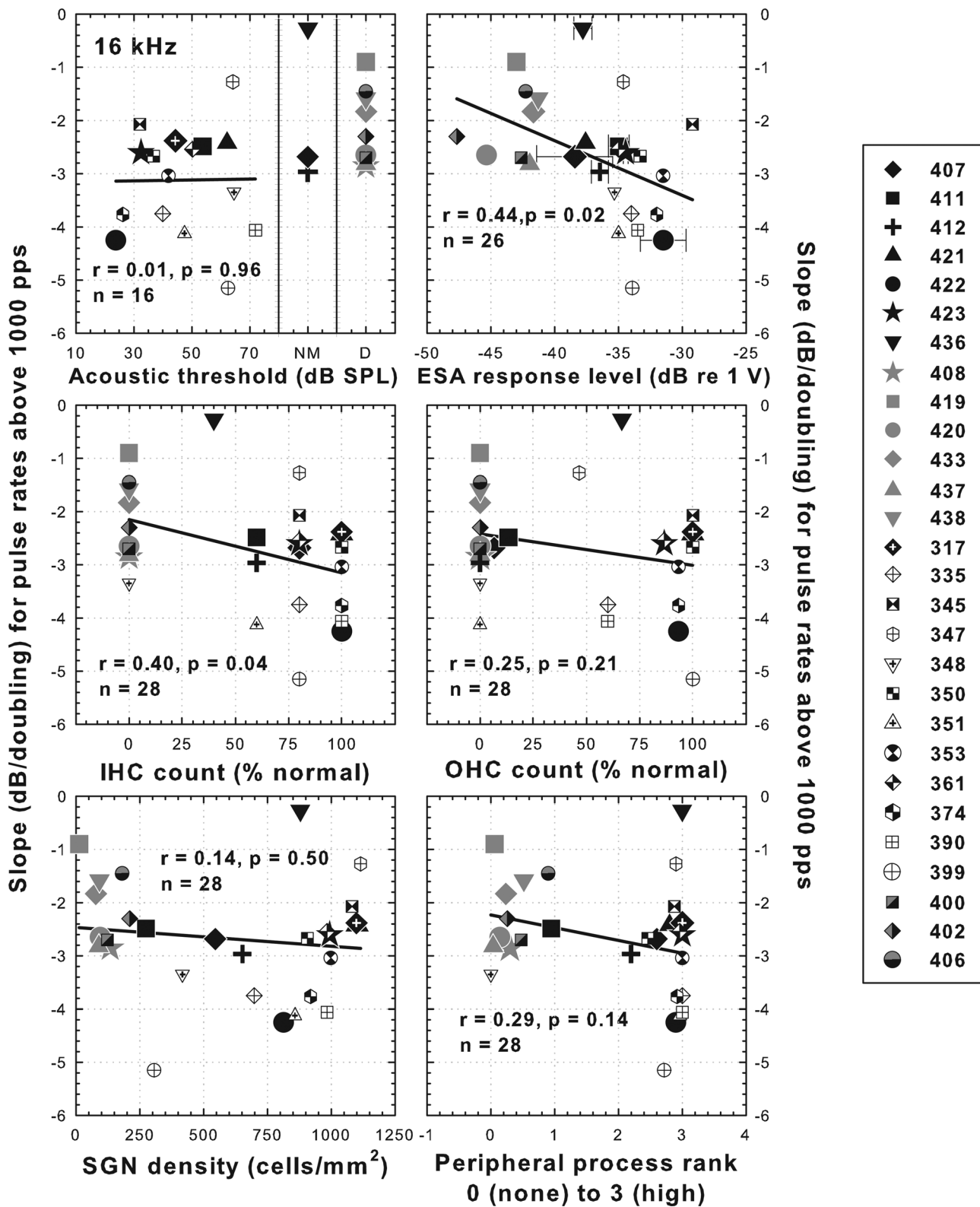


FIG. 9. Scatter plots comparing various measures of cochlear health with slopes of threshold versus pulse rate functions for 200 ms pulse trains at pulse rates above 1000 pps. Other details are as in Fig. 8.

The results of these studies are intriguingly reminiscent of experiments conducted by Gerken and colleagues (Gerken, 1979; Gerken *et al.*, 1991) although the conditions of those experiments were quite different. Gerken and colleagues studied psychophysical threshold versus stimulus duration functions for electrical stimulation of the cochlear nucleus (CN) and infe-

rior colliculus central nucleus (ICC) in cats and found that slopes of these functions decreased following cochlear damage induced by noise exposure or mechanical cochlear destruction. Interestingly the thresholds for CN and ICC electrical stimulation were lower for all stimulus durations following cochlear destruction (termed denervation hypersensitivity). Gerken and

colleagues concluded that the mechanism of temporal integration is based on neurons central to the inferior colliculus and that the mechanism is affected by conditions in the cochlea. The number of surviving auditory neurons and spontaneous activity in those neurons are both possible factors that could influence the central mechanisms of temporal integration.

### C. Relation of psychophysical measures to cochlear health

Of the 28 animals for which data are shown in Fig. 8, 11 had steep negative slopes of threshold versus pulse rate functions (larger than  $-1$  dB/doubling) at pulse rates below 1000 pps, indicative of multipulse integration. These animals all showed relatively high levels of cochlear health in the region of the implant as indicated by the presence of inner hair cells, peripheral processes, and relatively high spiral ganglion cell densities. All of these animals had some degree of preserved acoustic hearing in the tonotopic region near the implants and all had evidence of spontaneous activity in the auditory nerve. All but one (animal 351) had some preserved outer hair cells near the implant. However, we note that a few animals with relatively high levels of one or more of the indicators of cochlear health had shallow slopes for their threshold versus pulse rate functions. Furthermore, it is not possible to say which of these variables or combination of variables indicating cochlear health contributed to multipulse integration because the variables are all highly correlated with each other in this animal model (Table IV). An important future direction will be to develop an animal model with good spiral ganglion cell survival but no hair cells.

There are several potential mechanisms by which the presence of hair cells might affect multipulse integration. First, there is a potential for electrical stimulation of a cochlear implant to induce a traveling wave in the basilar membrane by causing contraction of outer hair cells or by a piezoelectric-like effect (Brownell *et al.*, 1985; Rabbitt *et al.*, 2005). If inner hair cells are intact, these phenomena could produce hearing mediated by stereocilia deflection and transmitter release similar to that produced by acoustic stimulation. In addition, it is possible that direct electrical stimulation of the inner hair cells could cause transmitter release and auditory nerve activation. Temporal and spatial properties of auditory nerve discharges in relation to the electrical signals mediated by these mechanisms would most likely be different from those elicited by direct electrical stimulation of the auditory nerve fibers. This might account for the differences seen between the animals with good versus poor cochlear health.

Another potential mechanism by which healthy inner hair cells in the implanted cochlea might affect multipulse integration is the generation of spontaneous activity in the auditory nerve. Spontaneous activity can have marked effects on the responsiveness to electrical stimulation by reducing abnormally high across-fiber synchrony and group refractory effects (Wilson *et al.*, 1997; Hu *et al.*, 2003). However, the known effects of spontaneous activity on synchrony of auditory nerve population responses occur at suprathreshold levels and are primarily seen at pulse rates

greater than 200 pps, so this specific mechanism is probably not applicable to the wide range of pulse rates tested in our experiment.

Data from human subjects cast some doubt on the idea that hair cells play important roles in determining the differences in multipulse integration observed across our animal population. In human subjects, we have found steep threshold versus pulse rate functions at low pulse rates in many cases including cases where there is no measurable acoustic hearing (Zhou *et al.*, 2011). These cases suggest that other variables might be contributing to the observed differences across subjects in multipulse integration. Spiral ganglion density is one possibility. Although spiral ganglion cell packing density is often correlated with hair cell survival, particularly in animal models, in humans SGN density is often relatively high even in the absence of hair cells (Hinojosa and Marion, 1983).

Of the animals represented in Fig. 8, all of the cases with relatively steep threshold versus pulse rate function slopes (steeper than  $-1$  dB/doubling) had relatively high SGN densities ( $> 600$  cells/mm<sup>2</sup>). However, several animals with shallow slopes also had relatively high SGN densities, suggesting that SGN density alone is not sufficient for good multipulse integration. Reduced sensitivity of the neurons to electrical stimulation, which can result from pathology that might not be obvious from the histological procedures that we used, could account for the results in these animals.

A simple model describing the relationship between pulse rate, detection thresholds, and SGN survival is that detection thresholds are dependent on the total spike count in the neural population (Botros and Psarros, 2010). In this model, the effectiveness of pulse rate in lowering thresholds would be greater in cases of good nerve survival because the effects of pulse rate on a single fiber would be multiplied by a greater number of nerve fibers than in cases of poor nerve survival. In this simple model, three factors would affect the total spike count in the surviving nerve-fiber population: the stimulus pulse rate, the number of surviving fibers, and the firing probabilities of the individual fibers. Only the first two variables are known for our experiment. The discharge probabilities of the individual fibers are not known but it is likely that they varied across subjects and across the population of surviving fibers within subjects. Responsiveness of the neurons is difficult to predict from their appearance in light microscopy. A low probability of discharge in the fibers could potentially account for the shallow threshold versus pulse rate functions observed in a few of the animals with high SGN densities.

A related consideration is that a subpopulation of auditory nerve fibers, such as the high-threshold, low-spontaneous-rate fibers, might be more susceptible to trauma than other subpopulations (Schmiedt *et al.*, 1996; Lin *et al.*, 2011). If the subpopulations are differentially sensitive to electrical stimulation, due, for example, to differences in fiber diameter, a selective loss of one type of fibers could change the aggregate response characteristics of the remaining population.

Considerations discussed in Sec. IV B suggest that the mechanism for multipulse integration resides in the auditory

pathway somewhere central to the inferior colliculus. However, we assume that the output of this integrator depends on the input received from neurons peripheral to the colliculus. The origin of across-subject differences in that input is likely to be the health of the implanted cochlea in the region of the electrode array. The fact that temporal integration varies across stimulation sites in human subjects with multisite electrode arrays (Donaldson *et al.*, 1997; Zhou *et al.*, 2011) is consistent with the idea that the origins of differences in multipulse temporal integration are in close proximity to the stimulation sites.

For pulse rates above 1000 pps, correlations of the slopes of the threshold versus pulse rate functions with the various anatomical and functional measures (Fig. 9) were weaker than those for pulse rates below 1000 pps seen in Fig. 8. Furthermore, across all of the cases reported here the slopes above 1000 pps were not significantly correlated with those below 1000 pps ( $r=0.053$ ,  $p=0.759$ ,  $n=36$ ). This suggests that the mechanisms underlying the slopes of the functions above 1000 pps must be different in some ways from those below 1000 pps and that they are less dependent on cochlear health. We have suggested that multiple mechanisms might be responsible for the slopes above 1000 pps including temporal integration combined with a residual partial-depolarization mechanism. However, it is not known if the temporal integration properties at pulse rates above 1000 pps are the same as those at the lower pulse rates so the relative contributions of these two components cannot be specified. The data in Fig. 9 suggest that differences in inner hair cell survival and spontaneous activity in the auditory nerve might influence these mechanisms.

In this study, as in the Kang *et al.* (2010) study, the cases with the steepest threshold versus pulse rate functions tended to have the lowest overall thresholds. In the combined data from the two studies, the correlation between threshold level at 156 pps and the slopes of the threshold versus pulse rate functions below 1000 pps was 0.66 ( $p=0.002$ ). This is probably due in part to differences across animals in multipulse integration. Nevertheless, thresholds for animals with the steepest threshold versus pulse rate functions were often lower than those for animals with shallow functions even for short duration stimuli or single pulses. On the other hand, several observations suggest that the relationship between slopes and levels of these functions is not causal. For example, in Fig. 2(A), thresholds for the 5 pps stimulus (one pulse in the 200 ms period) were nearly identical for animals 423, 419, and 433, but the slopes of the threshold versus pulse rate functions for these animals were very different at higher pulse rates. Similarly, in Fig. 4(A), two animals in the threshold versus stimulus duration experiment (423 and 433), had thresholds for one- and two-pulse stimuli that were nearly identical but the slopes of the temporal integration functions were markedly different. Absolute threshold levels at 156 pps were not well correlated with the histological and electrophysiological measures of cochlear health shown in Fig. 8. The correlation coefficients ranged from  $-0.002$  to  $-0.172$  and none were statistically significant ( $p \geq 0.4$ ).

## D. Clinical implications

In humans, pathology of deaf or hearing-impaired ears has been found to cover a very broad range in terms of measures such as presence of hair cells, peripheral processes and spiral ganglion cell neurons (Hinojosa and Marion, 1983; Nadol *et al.*, 1989; Incesulu and Nadol, 1998). The range of histopathology observed in humans is similar to that seen near the implant in the current study except that hair-cell survival in the region of the cochlear implant is rare in humans. With the broadening of inclusion criteria for implantation and with increasing efforts to preserve residual hearing, it is reasonable to expect more surviving hair cells in the region of the implant in the near future.

Currently the functional implications of this variation in cochlear health are poorly understood, as are the specific implications of improving conditions in the implanted cochlea. A few studies have suggested that hearing with cochlear implants is better in cases of poorer nerve survival and that a relatively small number of surviving spiral ganglion neurons are sufficient for a successful outcome of cochlear implant therapy (Fayad and Linthicum, 2006; Nadol *et al.*, 2001). However, one of the difficulties in relating human histopathology to cochlear implant function is that the histological data are usually gathered long after the functional measures are completed and possibly after a period of illness.

Non-invasive, clinically applicable measures such as the detection-threshold measures reported here are needed to assess cochlear health in conjunction with other measures of cochlear implant function. Accurate diagnosis of morphological conditions along the cochlear spiral could ultimately serve as a basis for choosing appropriate stimulation strategies as well as for selection of tissue engineering approaches to hearing rehabilitation on a patient specific basis.

Effects of temporal integration on stimulus detection are clinically important because the duration of information-bearing components of speech and other important acoustic signals vary considerably in duration. It would seem to be beneficial for temporal integration of electrical stimuli to be similar to that for acoustic stimuli. However, if the slopes of the temporal-integration functions are too steep, current levels that are comfortably loud for long-duration pulse trains might be very soft or inaudible for short duration stimuli.

Temporal integration slopes are known to vary across implanted human subjects and across stimulation sites within individual subjects (Shannon, 1989; Donaldson *et al.*, 1997; Zhou *et al.*, 2011). To the extent that these functions are indicative of cochlear health, they should reflect the temporal and spatial properties of neural input to central auditory processors. Thus they should reflect conditions that would affect more complex hearing functions. However, more research is needed to determine the specific functional significance of these slopes for perception of complex stimuli such as speech.

## ACKNOWLEDGMENTS

This work was supported by NIH/NIDCD Grants Nos. R01 DC007634, R01 DC004312, and P30 DC005188. We appreciate the contributions of Donald Swiderski and Lisa

Beyer for histological preparation, to Karin Halsey and David Dolan for ESA recordings, and to Ning Zhou for insightful comments on the manuscript.

<sup>1</sup>For animals implanted in a hearing ear, the variety of hair cell and nerve loss in the animals in part I of this study was larger than that for animals in the Kang *et al.* (2010) manuscript. This was probably due to the fact that the cable for the commercially supplied implants used in part I of this study was slightly longer than that for the implants in the Kang *et al.* study. The difference in the cable length made implantation slightly more difficult, probably resulting in more variation in insertion trauma and greater variety in hair cell and SGN loss.

<sup>2</sup>The background electrical noise for the ESA recordings reported in part I of this manuscript was somewhat different from that for the data reported in the Kang *et al.* (2010) manuscript. This is probably due to the fact that the data for part I of this manuscript were obtained after the laboratory had moved to a new building where the sources of electrical background noise were most likely different from those in the laboratory where the ESA data for Kang *et al.* (2010) were collected.

- Bierer, J. A. (2007). "Threshold and channel interaction in cochlear implant users: Evaluation of the tripolar electrode configuration," *J. Acoust. Soc. Am.* **121**, 1642–1653.
- Botros, A., and Psarros, C. (2010). "Neural response telemetry reconsidered: II. The influence of neural population on the ECAP recovery function and refractoriness," *Ear Hear.* **31**, 380–391.
- Brownell, W. E., Bader, C. R., Bertrand, D., and Ribaupierre, Y. (1985). "Evoked mechanical responses of isolated cochlear outer hair cells," *Science* **227**, 194–196.
- Dolan, D. F., Nuttall, A. L., and Avinash, G. (1990). "Asynchronous neural activity recorded from the round window," *J. Acoust. Soc. Am.* **87**, 2621–2627.
- Donaldson, G. S., Viemeister, N. F., and Nelson, D. A. (1997). "Psychometric functions and temporal integration in electric hearing," *J. Acoust. Soc. Am.* **101**, 3706–3721.
- Fayad, J. N., and Linthicum, F. H., Jr. (2006). "Multichannel cochlear implants: Relation of histopathology to performance," *Laryngoscope* **116**, 1310–1320.
- Galvin, J. J., 3rd, and Fu, Q. J. (2005). "Effects of stimulation rate, mode and level on modulation detection by cochlear implant users," *J. Assoc. Res. Otolaryngol.* **6**, 269–279.
- Galvin, J. J., 3rd, and Fu, Q. J. (2009). "Influence of stimulation rate and loudness growth on modulation detection and intensity discrimination in cochlear implant users," *Hear. Res.* **250**, 46–54.
- Gerken, G. M. (1979). "Temporal summation of pulsate brain stimulation in normal and deafened cats," *J. Acoust. Soc. Am.* **66**, 728–734.
- Gerken, G. M., Bhat, V. K. H., and Hutchison-Clutter, M. (1990). "Auditory temporal integration and the power function model," *J. Acoust. Soc. Am.* **88**, 767–778.
- Gerken, G. M., Solecki, J. M., and Boettcher, F. A. (1991). "Temporal integration of electrical stimulation of auditory nuclei in normal-hearing and hearing-impaired cat," *Hear. Res.* **53**, 101–112.
- Gfeller, K., Oleson, J., Knutson, J. F., Breheny, P., Driscoll, V., and Olszewski, C. (2008). "Multivariate predictors of music perception and appraisal by adult cochlear implant users," *J. Am. Acad. Audiol.* **19**, 120–134.
- Greenwood, D. D. (1990). "A cochlear frequency-position function for several species—29 years later," *J. Acoust. Soc. Am.* **87**, 2592–2605.
- Hinojosa, R., and Marion, M. (1983). "Histopathology of profound sensorineural deafness," *Ann. N. Y. Acad. Sci.* **405**, 459–484.
- Hu, N., Abbas, P., Miller, C., Robinson, B., Nourski, K., Jeng, F., Abkes, B., and Nichols, J. (2003). "Auditory response to intracochlear electric stimuli following furosemide treatment," *Hear. Res.* **185**, 77–89.
- Incesulu, A., and Nadol, J. B., Jr. (1998). "Correlation of acoustic threshold measures and spiral ganglion cell survival in severe to profound sensorineural hearing loss: Implications for cochlear implantation," *Ann. Otol. Rhinol. Laryngol.* **107**, 906–911.
- Kang, S. Y., Colesa, D. J., Swiderski, D. L., Su, G. L., Raphael, Y., and Pflugst, B. E. (2010). "Effects of hearing preservation on psychophysical responses to cochlear implant stimulation," *J. Assoc. Res. Otolaryngol.* **11**, 245–265.
- Lin, H., Furman, A., Kujawa, S. G., and Liberman, M. C. (2011). "Noise-induced primary neural degeneration in guinea pig: Does vulnerability depend on spontaneous discharge rate?" *Assoc. Res. Otolaryngol. Abstr.* **34**, 133.
- Middlebrooks, J. C. (2004). "Effects of cochlear-implant pulse rate and inter-channel timing on channel interactions and thresholds," *J. Acoust. Soc. Am.* **116**, 452–468.
- Middlebrooks, J. C. (2008). "Cochlear-implant high pulse rate and narrow electrode configuration impair transmission of temporal information to the auditory cortex," *J. Neurophysiol.* **100**, 92–107.
- Middlebrooks, J. C., and Snyder, R. L. (2007). "Auditory prosthesis with a penetrating nerve array," *J. Assoc. Res. Otolaryngol.* **8**, 258–279.
- Munson, B., and Nelson, P. B. (2005). "Phonetic identification in quiet and in noise by listeners with cochlear implants," *J. Acoust. Soc. Am.* **118**, 2607–2617.
- Nadol, J. B., Jr., Shiao, J. Y., Burgess, B. J., Ketten, D. R., Eddington, D. K., Gantz, B. J., Kos, I., Montandon, P., Coker, N. J., Roland, J. T., Jr., and Shallop, J. K. (2001). "Histopathology of cochlear implants in humans," *Ann. Otol. Rhinol. Laryngol.* **110**, 883–891.
- Nadol, J. B., Jr., Young, Y. S., and Glynn, R. J. (1989). "Survival of spiral ganglion cells in profound sensorineural hearing loss: implications for cochlear implantation," *Ann. Otol. Rhinol. Laryngol.* **98**, 411–416.
- Pflugst, B. E., Burkholder-Juhász, R. A., Xu, L., and Thompson, C. S. (2008). "Across-site patterns of modulation detection in listeners with cochlear implants," *J. Acoust. Soc. Am.* **123**, 1054–1062.
- Pflugst, B. E., and Xu, L. (2004). "Across-site variation in detection thresholds and maximum comfortable loudness levels for cochlear implants," *J. Assoc. Res. Otolaryngol.* **5**, 11–24.
- Pflugst, B. E., Xu, L., and Thompson, C. S. (2007). "Effects of carrier pulse rate and stimulation site on modulation detection by subjects with cochlear implants," *J. Acoust. Soc. Am.* **121**, 2236–2246.
- Rabbitt, R. D., Ayliffe, H. E., Christensen, D., Pamarthy, K., Durney, C., Clifford, S., and Brownell, W. E. (2005). "Evidence of piezoelectric resonance in isolated outer hair cells," *Biophys. J.* **88**, 2257–2265.
- Schmiedt, R. A., Mills, J. H., and Boettcher, F. A. (1996). "Age-related loss of activity of auditory-nerve fibers," *J. Neurophysiol.* **76**, 2799–2803.
- Searchfield, G. D., Munoz, D. J., and Thorne, P. R. (2004). "Ensemble spontaneous activity in the guinea-pig cochlear nerve," *Hear. Res.* **192**, 23–35.
- Shannon, R. V. (1989). "A model of temporal integration and forward masking for electrical stimulation of the auditory nerve," in *Cochlear Implant: Models of the Electrically Stimulated Ear*, edited by J. M. Miller and F. A. Spelman (Springer-Verlag, New York), pp. 187–203.
- Su, G. L., Colesa, D. J., and Pflugst, B. E. (2008). "Effects of deafening and cochlear implantation procedures on postimplantation psychophysical electrical detection thresholds," *Hear. Res.* **241**, 64–72.
- Wilson, B. S., and Dorman, M. F. (2008). "Cochlear implants: A remarkable past and a brilliant future," *Hear. Res.* **242**, 3–21.
- Wilson, B. S., Finley, C. C., Lawson, D. T., and Zerbi, M. (1997). "Temporal representations with cochlear implants," *Am. J. Otol.* **18**, S30–S34.
- Zhou, N., Xu, L., and Pflugst, B. E. (2011). "The effects of pulse rate on detection thresholds and maximum comfortable loudness levels in humans with cochlear implants," 2011 *Conference on Implantable Auditory Prostheses*—Abstract C32, p. 229.